Biochimica et Biophysica Acta 1788 (2009) 926–935

Contents lists available at ScienceDirect

Biochimica et Biophysica Acta

journal homepage: www.elsevier.com/locate/bbamem

Supramolecular organization of S12363-liposomes prepared with two different remote loading processes

Caroline Chemin [a,b,*], Jean-Manuel Péan [b], Claudie Bourgaux [a], Georg Pabst [c], Patrick Wüthrich [b], Patrick Couvreur [a], Michel Ollivon [a]

[a] Université Paris-Sud 11, UMR CNRS 8612, 5 rue J.B. Clément, 92290 Châtenay-Malabry, France
[b] Technologie SERVIER, 27 rue E. Vignat, 45000 Orléans, France
[c] Institute of Biophysics and Nanosystems Research, Schmiedlstrasse 6, Graz, 8042, Austria

ARTICLE INFO

Article history:
Received 28 June 2008
Received in revised form 27 October 2008
Accepted 11 November 2008
Available online 3 December 2008

Keywords:
Liposome
Spectrofluorimetry
Anticancer drug
Differential scanning calorimetry
X-ray diffraction
Active loading process

ABSTRACT

The S12363 anticancer drug was encapsulated into liposomes in an attempt to increase its therapeutic index. Loading of S12363 was achieved using two different processes based on the formation of either a pH gradient or an ammonium gradient between the acidic inner liposomal compartment and the basic outer phase. High encapsulation yields (>90%) were obtained using both processes for sphingomyelin/cholesterol/cholesterol-PEG vesicles. Spectrofluorimetry measurements have shown that liposomes were characterized by an internal pH around 4 for both loading processes. This internal pH was stable over a period of at least 20 days. Differential scanning calorimetry coupled with time-resolved synchrotron X-ray diffraction was used to study the drug/carrier supramolecular organization. In ammonium sulfate, S12363 was inserted into the bilayer in the vicinity of the polar headgroup. In citrate buffer, S12363 was mainly adsorbed at the water–lipid interface. The drug partitioning into the membrane was inhomogeneous and led to the formation of drug-rich and drug-poor domains. This effect was enhanced in the presence of cholesterol, especially in ammonium sulfate. To conclude, for both processes, the encapsulated drug was found inside the liposome aqueous core but strongly interacting with the membrane.

1. Introduction

Liposomes are simple lipid–bilayer vesicles useful as drug-delivery systems. Liposomes were already suggested as drug carriers in cancer chemotherapy by Gregoriadis et al. in 1974 [1]. Since then, their interest in tumor treatment has increased tremendously. Indeed, the encapsulation of anticancer drugs within lipid vesicles has been shown to decrease toxic side effects while increasing or maintaining therapeutic activity. The drug substance S12363 is a vinca alkaloid derivative, synthesized by grafting an optically active α-aminophosphonate on O4-deacetyl vinblastine (Fig. 1) [2]. This compound was evaluated for cytotoxic and antitumor activity against a spectrum of murine and human tumors and was found to be on average 72 and 36 fold more cytotoxic than vincristine and vinblastine respectively [3]. Unfortunately, this drug had a very low therapeutic index, the efficient dose being close to that of toxicity; lethal dose 10 was 40 mg/kg in mouse. Therefore, S12363 was encapsulated into long-circulating liposomes to take advantage of the so called "Enhanced Permeability and Retention" (EPR) effect, and to improve the therapeutic index of the compound [4,5].

The encapsulation procedure has been chosen on the basis of the physico-chemical properties of the drug substance. Indeed, S12363 is a weak base with a pH-dependent aqueous solubility and lipophilic profile. Thus, active loading process, based on the formation of either a pH gradient [6] or an ammonium gradient [7] between the acidic inner liposomal compartment and the basic outer phase, was used to load S12363 into liposomes. Since the drug substance was highly soluble in acidic medium and poorly soluble in a neutral/basic environment, the drug accumulated inside the vesicles. Actually, high encapsulation yields (>90%) were obtained using both gradients for sphingomyelin/cholesterol/cholesterol-PEG (ESM/Chol/Chol-PEG) vesicles composition. Liposomes formed with the encapsulated S12363 drug were stable for weeks. The lipid–bilayer composition of the liposome has been chosen for i) the high stability of ESM in acidic conditions and ii) the property of Chol to condense ESM bilayers more

Abbreviations: Chol, cholesterol; Chol-PEG, pegylated cholesterol; DLS, dynamic light scattering; DPPC, dipalmitoyl phosphatidylcholine; DSC, differential scanning calorimetry; EPR effect, enhanced permeability and retention effect; ESM, egg sphingomyelin; MLVs, multilamellar vesicles; LUVs, unilamellar vesicles; OrG, Oregon green; PBS, phosphate buffer saline; PEG, polyethylene glycol; SAXS, small angle X-ray scattering; T_m, melting temperature; T_{onset}, onset of the transition temperature; XRDT, X-ray diffraction as a function of temperature; WAXS, wide angle X-ray scattering; ΔH, fusion enthalpy

* Corresponding author. Université Paris-Sud 11, UMR CNRS 8612, 5 rue J.B. Clément, 92290 Châtenay-Malabry, France. Tel.: +33 2 38 23 8000.
E-mail addresses: caroline.chemin@u-psud.fr, caroline.chemin@fr.netgrs.com (C. Chemin).

0005-2736/$ – see front matter © 2008 Elsevier B.V. All rights reserved.
doi:10.1016/j.bbamem.2008.11.017

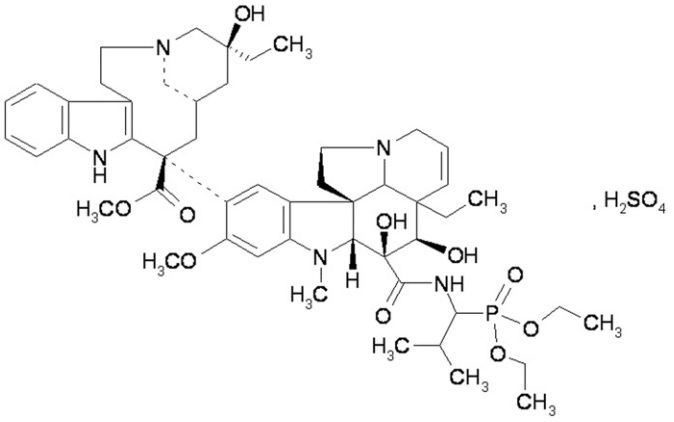

Fig. 1. Developed formula of sulfate S12363 or diethyle of (1S)-1-[(O4-deacetyl-3-demethoxycarbonyl vincaleucoblastin-3-yl)-carbonylamino]-2-methyl propyl phosphonate ($C_{51}H_{72}N_5O_{10}P$, H_2SO_4). Molecular weight 1044.2 g/mol (946.144 + 98.078).

tightly and to desorb slowly from such bilayers [8] which results in lower permeability of such bilayers [9,10]. This bilayer composition has been already used for similar drugs [11,12]. Furthermore, pegylated cholesterol has been added to the liposomes bilayer to obtain prolonged blood circulation of liposomes [4].

In such drug carrier the association between the drug and the lipid vesicle is directly correlated with the encapsulation efficiency and with the release profile. Previous studies have found that the leakage of S12363 from liposomes was mainly dependent upon the sample dilution, a "burst effect" being observed in certain conditions [13]. Such phenomenon has not yet received interpretation but it is suspected that the drug retention depends markedly on its interactions with the liposomal membrane. Understanding the interactions between the drug substance and the membrane bilayer is of prime importance for the design of efficient drug carrier vesicles because if the release rate of the biologically active substance is more rapid than the kinetic of tissue accumulation, then the therapeutic activity may be compromised [4,14]. The detailed study of S12363 interactions with lipids may lead to an improved design of liposome formulation for most efficient drug delivery.

The aim of this study was to identify the location of the S12363 drug substance into the liposome, depending on the loading procedure used. In order to get this information, liposomal internal pH has first been measured by spectrofluorimetry measurements using an appropriate pH probe and appearance of liposomes has been studied by cryotransmission electron microscopy. Then, phospholipid–drug molecular interactions have been investigated by Differential scanning calorimetry (DSC) and by Small and Wide Angle X-ray Diffraction (SWAXS) in medium corresponding to the liposome formulation and using different lipid compositions. DSC is a sensitive method to study the thermotropic phase behavior of lipid membranes [9,15–17] and any interaction between the S12363 drug and the bilayer modeling liposome membrane, would lead to a modification of the thermodynamic parameters (temperature of the melting transition T_m and corresponding fusion enthalpy ΔH). The structural parameters would also be modified by the drug/membrane interactions thus X-ray diffraction provides complementary information [18,19].

2. Materials and methods

2.1. Materials

S12363 sulfate was obtained from the Institut de Recherche Servier (IDRS, Suresnes, France), S12363 citrate and its corresponding base were obtained from Technologie Servier (TES, Orléans, France). Egg sphingomyelin (ESM) was purchased from Avanti Polar Lipids (Alabaster, AL, USA), cholesterol (Chol) from Sigma (St. Louis, MO, USA) and pegylated cholesterol (Chol-PEG_{5000}) from Nof Corporation (Japan). Oregon Green (OrG) was obtained from Invitrogen (Cergy Pontoise, France). The ESM utilized was highly enriched in long-chain saturated fatty acids, particularly in 16:0 (84%) and contained only small amounts of 18:0 (6%), 20:0 (2%), 22:0 (4%) and 24:0 (4%). Purified water was used for sample and buffer preparations.

2.2. Liposome preparation and S12363 encapsulation

ESM, Chol and Chol-PEG_{5000} (50:45:5 molar ratio) were dissolved and mixed in ter-butanol at 60 °C and then freeze-dried (CRIST, Bioblock Scientific). The lyophilized mixture was hydrated with either citrate buffer 200 mM pH 3 (pH gradient) or ammonium sulfate 155 mM pH 5.2 (ammonium gradient) and heated at 60 °C during 20 min. The suspension was subjected to five freeze–thaw cycles. The resulting MLVs were then extruded through a Lipex® extrusion device (Northern Lipids) equilibrated at 60 °C and under nitrogen pressure. The extruder was fitted with polycarbonate filters with successive pore size of 0.8 μm, 0.4 μm, 0.2 μm and 0.1 μm. Resulting LUVs mean diameter was estimated by quasi-elastic light scattering (Nanophox, Sympatec) using the "unimodal" method of data processing. In the case of pH gradient, LUVs were incubated with S12363 and the gradient was formed by adding TRIS buffer and by increasing the external pH of the citrate buffer to 6.8 with NaOH. The suspension was mixed for 30 min at room temperature and 5 min at 70 °C. Finally, the external pH was increase to 8 and a dilution was realized to have an iso-osmotic suspension. To create the ammonium gradient, liposomes were passed through a Hi-Prep desalting column pre-equilibrated with glucose 5% in order to remove external sulfate ammonium salts. S12363 was incubated with LUVs at room temperature for 15 min and then at 60 °C for 20 min. The pH was fixed at 6. The encapsulation efficiency was determined by separating the entrapped drug from the free by a gel exclusion chromatography through a Sephadex G75 column pre-equilibrated with the corresponding medium (citrate buffer + TRIS buffer pH 8 or Glucose 5%). S12363 was followed by UV spectroscopy at 230 nm. The dosage of the encapsulated fraction was done by HPLC and the drug/phospholipid weight ratio was 1:35. The rate of liposome drug uptake was more than 90% in both cases and formulations were stable at 4 °C for at least 1 month.

2.3. Spectrofluorimetry measurements

In order to determine the pH of liposome core, a pH probe Oregon Green (OrG) was encapsulated [20]. The OrG pH probe was solubilized in the appropriate medium (citrate buffer or ammonium sulfate solution) at 10^{-4} M before lipid hydration. Then, liposomes were formed as described in previous section. Liposomes were separated from free OrG by gel exclusion chromatography on Sephadex® G50 150–100 G (Sigma). The system was composed of a peristaltic pump (Pharmacia LKB-Pump P-1), a six-way PTFE injection valve (Rheodyne, type 50, Interchim, France), a 0.5 ml injection loop (Daka Ware, Chicago, USA), a glass column (height = 27 cm, DIAMETER = 1 cm) containing the gel swollen in the appropriate buffer, a 10 μl circulation quartz cuvette (no. 010, Hellma, Germany) and a fraction collector (Microcol, Gilson TDC80, Villiers le Bel, France). Elution was carried out at a flow-rate of 0.3 ml min^{-1} using either citrate buffer pH 8 (pH gradient) or Glucose 5% (ammonium gradient) as the mobile phase and 1 ml fractions were collected. The elution of OrG liposomes and free OrG was monitored by measuring the fluorescence with a four-channel fluorimeter Spex F1T11I (equipped with Peltier-cooled photomultipliers and a 450 W xenon lamp) controlled by DM 3000 software (Spex Industries, Edison, USA). Fluorescence emission was measured at 90°. Samples were maintained at 20 °C by a water bath (Lauda RCS6, Lauda, Königshafen, Germany). OrG elution was monitored at 555 nm after excitation at 488 nm, while liposomes

were detected at the same time by light scattering at 488 nm. Liposomes without external OrG were subjected to an emission scan between 400 and 540 nm with excitation at 488 nm. Calibration was done in the appropriate buffer as a function of pH which is directly correlated with the ratio of the fluorescence intensity measured at 504 nm and at 466 nm (Fig. 2).

2.4. DSC and X-ray sample preparation

Samples (about 20 mg of anhydrous lipids) were prepared by dissolving and mixing the indicated lipids in ter-butanol at 60 °C to obtain the desired composition. The samples were then freeze-dried at $P<1$ mbar and $T=-35$ °C and the lipid mixture obtained was hydrated with water, citrate buffer (200 mM) pH 4 or ammonium sulfate (155 mM) pH 4. Citrate buffer pH was increased with sodium hydroxide (32%) and ammonium sulfate pH was decreased with sulfuric acid (1 N). The final concentration of lipids was 200 mg/ml. The molar sterol concentrations were 0, 10 or 40 mol%. S12363 was solubilized in citrate buffer or freeze-dried with lipids before hydration with water or ammonium sulfate. Chol-PEG was not added into the membrane model in order to have well defined X-ray patterns. These suspensions were heated above the chain melting transition temperature of ESM and vortexed in order to ensure good sample homogeneity. Using single use syringes equipped with long needles, an aliquot of the samples was then loaded into DSC hermetically sealed aluminum pans (TA Instruments) and quartz capillaries (external diameter ≤ 1.5 mm and wall thickness = 0.01 mm) (GLAS, Müller, Berlin, Germany). Low-speed centrifugations (<1000 rpm) were used to concentrate the lipidic phase down to the bottom of the capillary. The top of the capillary was closed by a drop of melted paraffin to prevent water evaporation. The suspensions phase separate into lipidic rich moiety and clear water or buffer moiety, thus demonstrating full hydration. Before analyses, DSC pans and capillaries were kept at 4 °C during at least one night and at most one weak.

2.5. Differential scanning calorimetry

Differential scanning calorimetry (DSC) measurements were performed in a Q1000 DSC, TA Instruments. Heating scans were run from 10 °C to 60 °C at a heating rate of 2 °C/min. An empty hermetically sealed aluminum pan was used as reference. The calorimeter was calibrated using lauric acid as standard reference sample ($\Delta H = 178.3$J/g, $T_m = 43.7$ °C). Protocol of standardization by lauric acid, which is a lipid with thermal properties close to those of ESM, is described by Grabielle-Madelmont and Perron [21]. Data analysis was performed using the TA Universal Analysis program. The transition temperatures were taken at the onset of the transition (T_{onset}), i.e., at the intercept of the tangent to the low-temperature side of the thermal peak with the baseline. The transition enthalpy changes were obtained from the area under the peak and standardized by the mass of the phospholipid. To calculate the area under the peak, the baseline was formed by connecting the linear segments of the heat capacity curve between the start and endpoint of the transition.

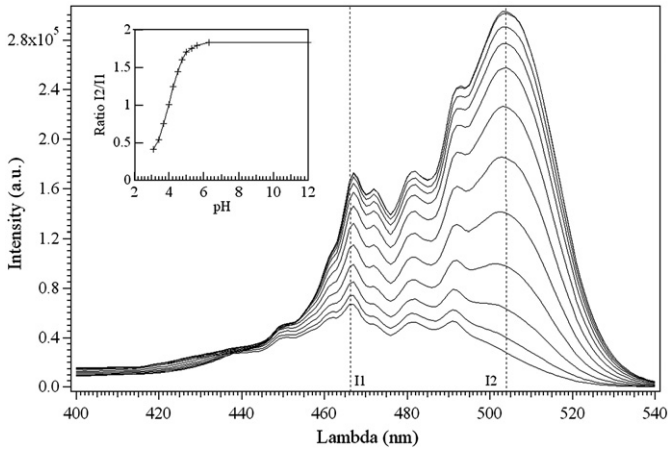

Fig. 2. Calibration with Oregon green (1.5 mM) in citrate buffer 200 mM from pH 3 (bottom) to pH 12 (top). Citrate buffer pH was increased with NaOH 32%. OrG was subjected to an emission scan between 400 and 540 nm with an excitation at 488 nm. The pH is directly correlated with ratio of the fluorescence intensity measured at I2 = 504 nm and at I1 = 466 nm (insert).

2.6. X-ray diffraction as a function of temperature

X-ray small and wide angle diffraction measurements were carried out using a monochromatic focused X-ray beam (0.8 × 0.8 mm) on the Austrian SAXS beamline at ELETTRA, Trieste, Italy (H. Amenitsch, http://www.ibr.oeaw.ac.at/beamline/index.html). For all of the experiments a calorimeter sample holder (MICROCALIX) which allows X-ray diffraction patterns to be recorded as a function of temperature (XRDT), developed by Keller et al. [22], was used. Simultaneous small-angle (SAXS) and wide-angle (WAXS) X-ray scattering intensities of the diffraction lines were recorded using two one dimensional position-sensitive linear detectors (1024 channels, filled with argon–ethane mixture). The calibration of the detectors was performed with crystalline β form of highly purified tristearin (repeat distance of 44.95 ± 0.05 Å at small angles and 4.59, 3.85, 3.70 ± 0.01 Å at wide angles) [23]. X-ray data and DSC thermal measurements were synchronously collected versus time by a National Instrument LabVIEW supported data acquisition system (H. Amenitsch, HCI, Hecus X-ray Systems, Graz, Austria). DSC-XRDT scanning rate were performed at 2 °C/min with a time frame of 30 s (1 frame/°C) at either 8 keV or 16 keV.

2.7. Global analysis technique

Selected SAXS patterns in the gel and in the fluid phase of ESM and ESM/Chol mixtures water, in citrate buffer at pH 4 and in ammonium sulfate solution at pH 4 were analyzed in terms of a global model [24,25] using the program GAP (Global Analysis Program). The analysis technique models the full q-range in the SAXS regime including Bragg peaks and diffuse scattering (for recent review see Pabst et al., 2006 [26]). The major advantage of this model is its ability to retrieve structural information for all lamellar aggregation forms including unilamellar, oligolamellar and multilamellar vesicles using a single description of the bilayer's electron density profile. From the analysis, we obtained the membrane thickness through the definition $d_B = 2(z_H + 2\sigma_H)$, where z_H was the position of the headgroup Gaussian modeling the electron density profile and σ_H its width. The bilayer separation was then simply given by $d_W = d - d_B$.

2.8. Cryo-transmission electron microscopy (c-TEM)

The cryogenic transmission microscopy investigations were performed with a Cryo-EFTEM LEO-Zeiss 912 at the "Service de Microscopie Electronique de l'Institut de Biologie Intégrative" (IFR 83 CNRS, Paris). Liposomes were prepared as described above and were stored at 4 °C for approximately 1 week prior to obtain the cryo-images. Samples (2–5 μL) of both formulations (pH gradient and ammonium gradient) of S12363 loaded and S12363 unloaded liposomes were deposited on a Formvar/carbon coated copper grids. Excess liquid was thereafter blotted away with filter paper. The samples were quickly vitrified by plunging them rapidly into liquid ethane bath cooled by liquid nitrogen (LEICA EM CPC, Vienna, Austria). To prevent sample perturbation and the formation of ice crystals, grids were kept below 108 K during both the transfer and viewing procedures. All observations were made in zero-loss bright-field mode at an accelerating voltage of 120 kV. Note that the two-dimensional projection of a closed liposome will appear as a circular object with enhanced contrast around the rim. This is due to

the fact that the projected thickness of the bilayer shell is maximum at the edge.

2.9. Liposome stability and drug leakage

Liposome stability was evaluated by measuring the drug fraction still encapsulated after 1 month at +4 °C. To evaluate the drug release, S12363-liposomes prepared by either pH gradient or ammonium gradient were diluted 1:100 in PBS pH 7.4 and incubated at 37 °C during 30 min. The encapsulated fraction was determined by separating the entrapped drug from the free by a gel exclusion chromatography through a Sephadex G75 column pre-equilibrated PBS pH 7.4. S12363 release was followed by UV spectroscopy at 230 nm. The dosage of the encapsulated fraction was done by HPLC.

3. Results and discussion

3.1. Internal pH of liposomes

Liposomes were prepared either in citrate buffer pH 3 or in ammonium sulfate pH 5.2. In the first case the pH gradient was formed by increasing the external pH of citrate buffer to 8. In ammonium sulfate, an ammonium gradient was induced by removing external salts (see Section 2). Noteworthy, in the absence of a gradient between the external and internal core, it was impossible to load significant amount of S12363 into liposomes. The drug remained in the ammonium sulfate solution in the external phase and only a weak part of the drug interacted with the liposome membrane.

The mean diameter of the liposomes was measured by DLS and yielded an average value of 170 +/− 10 nm in both cases. The liposomes size and external pH were stable over several months. Nevertheless the inner pH of the liposomes at the moment of the gradient formation as well as the gradient stability was unknown. Regarding the properties of the drug this parameter is the most important for the supramolecular organization of the S12363-liposome. Indeed, S12363 is a weak base highly soluble in acidic medium and poorly soluble in a neutral/basic environment (Fig. 3). These properties determine the affinity of the drug substance with the core or the liposome membrane. Furthermore the pH gradient persistence is correlated with the S12363-liposome stability.

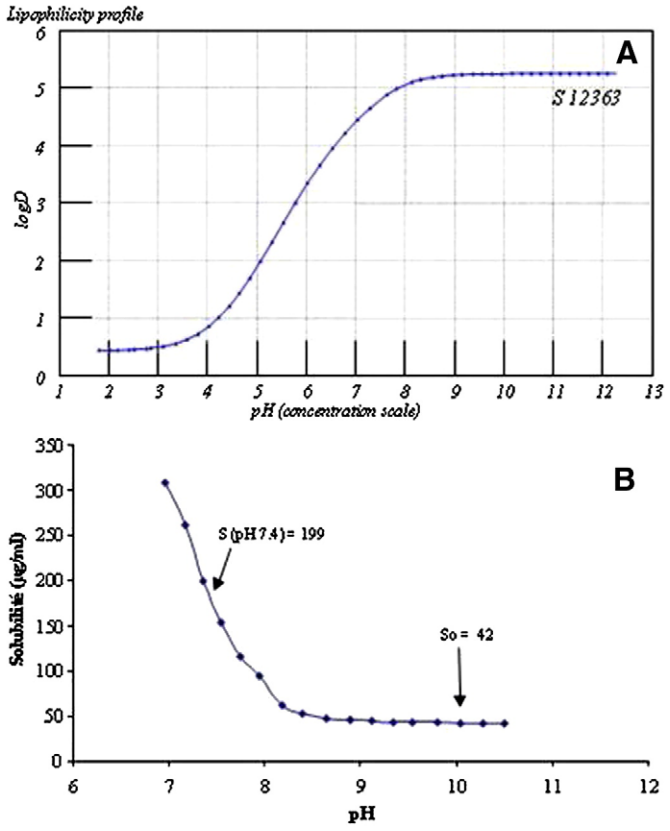

Fig. 3. Lipophilic (A) and solubility (B) profiles of S12363 sulfate as a function of pH.

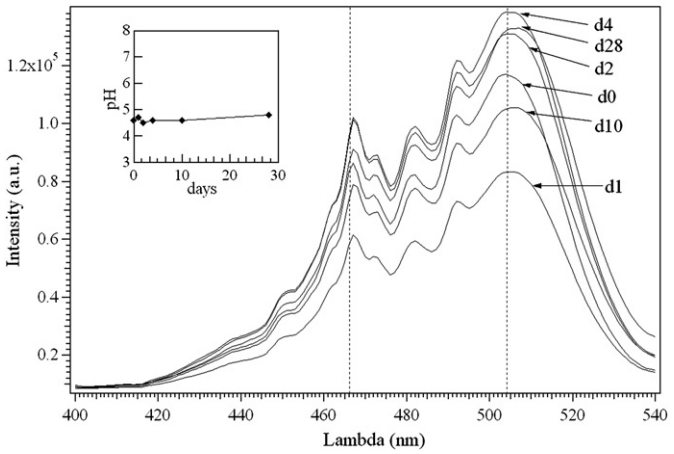

Fig. 4. Emission scans of the pH probe Oregon Green encapsulated in liposomes as a function of time (λex = 488 nm). The liposomes were prepared in citrate buffer pH 3. The scan at day 0 (D0) was done just after external pH increase (see Materials and methods) and after a gel exclusion chromatography was done to remove the external probe. Then, liposome core pH was measured 1, 2, 4, 10 and 28 days after this increase. In all cases a gel exclusion chromatography was done before the emission scan. The internal pH is directly correlated with the ratio of the fluorescence intensity measured at wavelength 504 and 466 nm. The insert shows the evolution of the pH liposome core as a function of time.

For this purpose a pH probe (Oregon Green) has been encapsulated into the vesicles (see Section 2). In the case of liposomes prepared in citrate buffer, the internal pH was measured before the increase of the external pH and was found to be 3.1. This result was in accordance with the expected value of 3 and showed that Oregon Green was an appropriate probe for pH determination in vesicle core. After external pH increase, the internal pH reached a value of 4.6 (Fig. 4). This pH was then stable over a period of at least 28 days. In the case of liposomes prepared in ammonium sulfate, the internal pH was measured just after external salts removal (Fig. 5). The internal pH reached a value of 3.8 and was stable over a period of at least 20 days.

As these experiments were realized with unloaded liposomes, S12363 was then solubilized in citrate buffer pH 4 and in ammonium sulfate pH 4 at a concentration corresponding to the complete drug solubilization in the aqueous core of the liposomes. To determine this concentration, the trapped volume of vesicle preparations was estimated as described previously [27,28], that is the internal volume, V_{int} = 5 µL/µmol of phospholipids for 170 nm liposomes. In the present case a suspension of 8 mg/mL in lipids with an average FW of 1023.7 represents 7.815 µmol/mL of lipids and therefore a trapped volume in the liposome suspension of 39.075 µL/mL. Since the drug concentration in the liposome suspension was 0.2 mg/mL, the estimated concentration in the liposome core was 0.2/0.039 = 5.1 mg/mL.

In citrate buffer, no pH variation was seen in the presence of the drug substance solubilized at 5.1 mg/mL. In ammonium sulfate the drug was not completely soluble at the same concentration and the pH was increased from 4 to 6. This difference in drug solubility between the two media was attributed to the buffer effect of the citrate buffer and indicates that in the case of the ammonium gradient, part of the drug could precipitate in the liposome interior.

3.2. Cryo-TEM

Since the formation of an insoluble precipitate in the liposome core has shown previously to decrease the drug release in case of

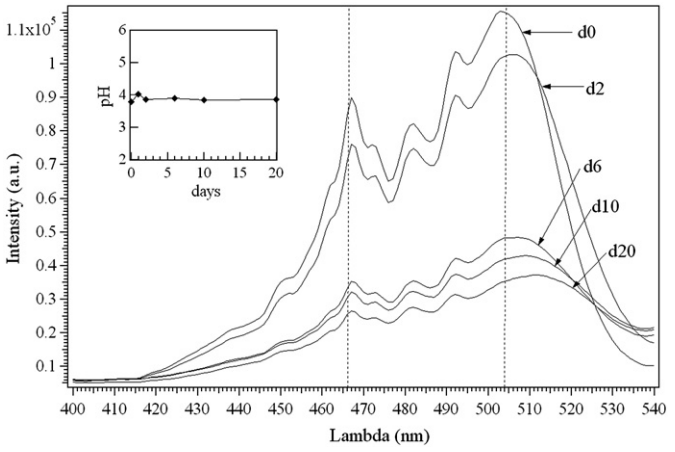

Fig. 5. Emission scans of the pH probe Oregon Green encapsulated in liposomes as a function of time (λex = 488 nm). The liposomes were prepared in ammonium sulfate pH 5.2. The scan at day 0 (D0) was done just after external salt removing (see Materials and methods) and after a gel exclusion chromatography was done to remove the external probe. Then, liposome core pH was measured 2, 6, 10 and 20 days after this increase. In all cases a gel exclusion chromatography was done before the emission scan. The internal pH is directly correlated with the ratio of the fluorescence intensity measured at wavelength 504 and 466 nm. The insert shows the evolution of the pH liposome core as a function of time.

doxorubicin formulation [29], it was consequently important to determine if a drug precipitation following S12363 loading occurred in the case of NH_3-gradient formulation. Liposome appearance was determined by cryo-TEM with either a pH gradient or with a NH_3-gradient with and without S12363 encapsulated. Images are shown in Fig. 6. Liposomes had spherical morphology and were mostly uniform in size. The interior of S12363-loaded liposomes exhibited the same electron density compared with unloaded liposomes whatever the loading process used. The drug precipitation in the liposome core previously observed with doxorubicine [29], topotecan [30] or suspected with vinca alkaloid [31] was not evidenced with S12363-liposomes, maybe because of a lower drug-to-lipid ratio (between 5 and 10 fold) but more probably because S12363 was, at least partly, embedded in the membrane.

3.3. Interactions between S12363 and liposome bilayer

DSC/X-ray measurements were performed to observe interactions between the drug substance S12363 and the liposome bilayer. The X-ray diffraction patterns were recorded at wide angles to get information about the packing of the phospholipid hydrocarbon chains and at low angles to obtain the long-range organization of the lipid assemblies. To determine the impact on DSC-XRDT profiles of a complete drug insertion into the membrane, S12363/bilayer interactions were first studied in purified water in which S12363 was not soluble. Interactions between S12363 and the liposome bilayer were then determined in the medium corresponding to the liposome core, i.e., in citrate buffer or in ammonium sulfate at pH 4. Interactions between S12363 and the lipid membrane have been determined without cholesterol to get information about the behavior of the drug substance in presence of ESM alone and with 10 and 40 mol% of Chol to see the influence of Chol content on drug/bilayer interactions.

3.3.1. Drug/liposome bilayer interactions in water

Thermodynamic parameters of the main phase transition are directly correlated with ESM chain melting. These parameters were influenced by the insertion of the drug in ESM bilayers and variations

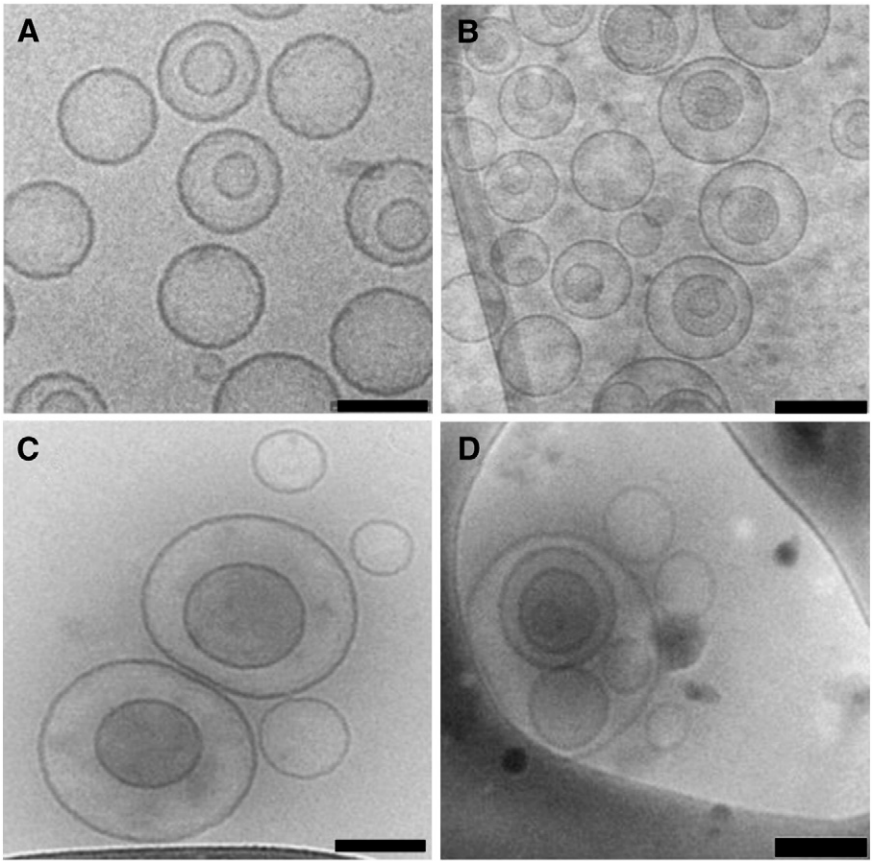

Fig. 6. Cryo-TEM micrographs of liposomal formulations. Liposomes were prepared either by pH-gradient (A and B) or by NH_3-gradient (C and D). (A and C) Liposomes in the absence of drug, (B and D) liposomal S12363 at a drug/lipid weight ratio of 1/35. The size bar represents 100 nm.

were found concentration dependent (Fig. 7). Indeed, increasing the drug concentration into the bilayer induced a decrease of both the melting enthalpy (Fig. 7A) and the melting temperature (Fig. 7B). The melting temperature was decreased from 39.3 °C without drug to 36.7 °C with the highest drug/ESM molar ratio of 0.07, and the melting enthalpy was decreased from 6.25 kcal/mol without drug to 4.35 kcal/mol with the drug/ESM ratio of 0.07 (drug/lipid weight ratio = 1/10). These results are consistent with a possible insertion of S12363 into the bilayers. Moreover, the phase transition was wider and a shoulder was observed on the high temperature side of the peak in the presence of the drug (Fig. 8A, right side).

The melting transition was also identified by X-ray diffraction. The wide angle diffraction patterns showed the existence of a transition from an ordered to a disordered chain packing in the plane of the bilayer. X-ray pattern at 20 °C of pure ESM bilayers hydrated with purified water displayed a ripple lamellar gel phase $P\beta'$ with a d-spacing of 65.4 Å and a broad wide angle line at 4.17 Å [32]. The insertion of S12363 into the bilayers (molar ratio of 0.07) led to the disappearance of the characteristic peak of the ripple phase at small angles whereas the lamellar gel phase had a similar d-spacing (Fig. 8A). The broad WAXS line at 4.17 Å showed that the hexagonal chain packing was maintained. These observations suggested that a gel phase with tilted hexagonally packed chains but without modulation was formed in the presence of the drug. At 55 °C, the lamellar d-spacing of the liquid crystal phase increased slightly (+2.4 Å) due to an increase in d_W (Fig. 8A and Table 1).

In the presence of 10 mol% of cholesterol, the thermodynamic parameters with and without S12363 were markedly different (Fig. 7). In the presence of the drug (molar ratio of 0.07), the melting transition was wider, the onset temperature was decreased and the presence of a small second endotherm at higher temperature led to an offset temperature close to those of ESM/Chol bilayers alone (Fig. 8, right side). The melting enthalpy was also decreased. The lamellar structure was preserved whatever the temperature. Nevertheless, the drug compound insertion induced a decrease of the d-spacing of the lamellar gel phase L_β, from 73 Å to 71 Å and an increase in the d-spacing of the liquid crystalline phase L_α from 63 Å to 66 Å. Electron density profiles showed that these variations are due to changes of the interbilayer water thickness (Table 1). Electron density profiles were similar in the glycerol backbone-headgroup regions but differed markedly throughout the region of the hydrocarbon tails (Fig. 9A and B). This confirmed that drug molecules were embedded in the bilayer.

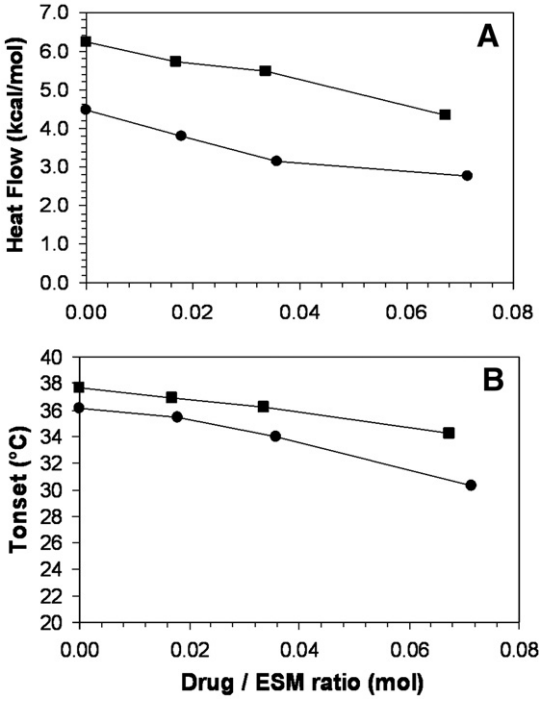

Fig. 7. Fusion enthalpy (A) and temperature variation (B) of the chain melting transition of ESM fully hydrated with water as a function of the drug/ESM molar ratio. (■) ESM bilayers without cholesterol; (●) ESM bilayers with 10 mol% of cholesterol.

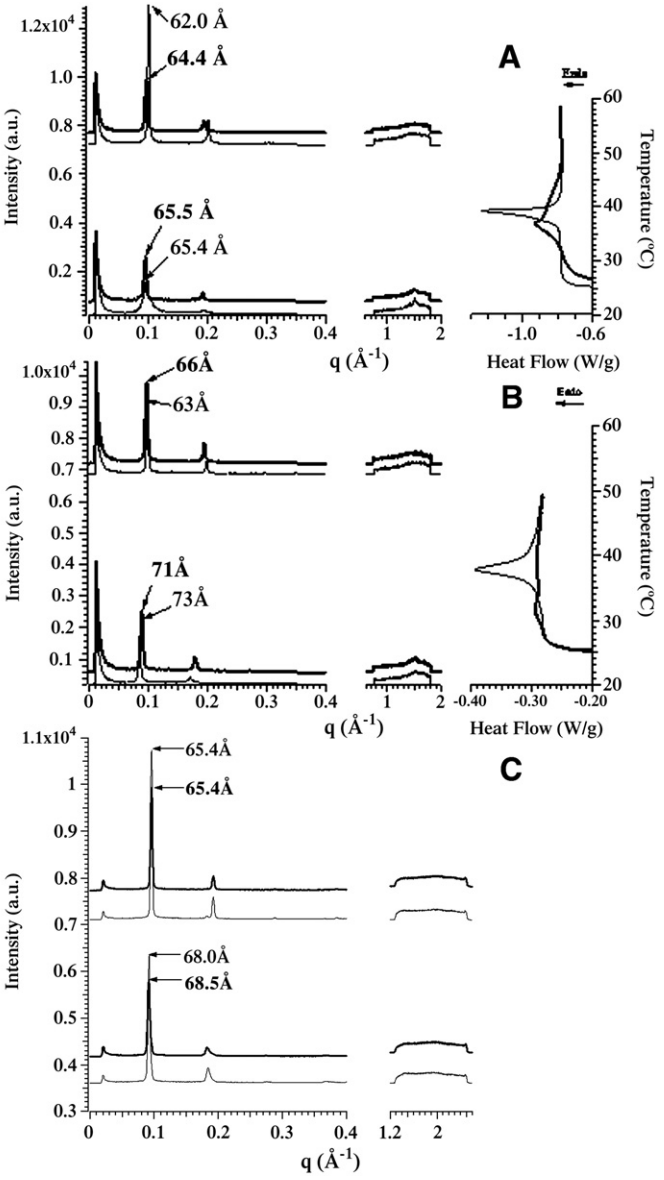

Fig. 8. SWAXS diffraction patterns (left) at 20 °C (bottom) and 55 °C (top) of bilayers hydrated with purified water. (A) ESM bilayers (plain curves) or ESM/S12363 bilayers (bold curves) (B) ESM/Chol (90:10) bilayers (plain curves) or ESM/Chol/S12363 bilayers (bold curves). (C) ESM/Chol (60:40) bilayers (plain curves) or ESM/Chol/S12363 bilayers (bold curves).The right part shows corresponding DSC curves (scanning rate 2 °C/min).

In the presence of 40 mol% of cholesterol, the calorimetric signal was too weak to be integrated and was well correlated with the absence of WAXS peaks at all temperatures. The insertion of S12363 in the bilayer containing 40 mol% of Chol induced a weak increase of the lamellar repeat period (0.5 Å) at 20 °C and no effect was seen at 55 °C (Fig. 8C).

3.3.2. Drug/liposome bilayer interactions in citrate buffer

The melting temperature, observed by DSC, occurred at lower temperature in the presence of S12363 and the peak was wider because of the occurrence of a shoulder on its high temperature side. However, the fusion enthalpy was not decreased by the presence of

Table 1
Influence of S12363 on the bilayer thickness (d_B) and the water layer thickness (d_W) of ESM and ESM/Chol (90:10) bilayers at 20 °C and 55 °C and fully hydrated with water, citrate buffer pH4 or ammonium sulfate solution pH4.

				Water	Citrate buffer pH4	Ammonium sulfate pH4
ESM	Without drug	20 °C	d_B	–	–	–
			d_W	–	–	–
		55 °C	d_B	48.4	49.6	48.2
			d_W	14.3	16.2	29.0
	S12363	20 °C	d_B	–	–	–
			d_W	–	–	–
		55 °C	d_B	48.3	47.5	48.2
			d_W	15.9	26.1	32.5
ESM/Chol 90:10	Without drug	20 °C	d_B	54.1	56.6	55.7
			d_W	19.2	18.7	26.1
		55 °C	d_B	53.5	51.3	49.5
			d_W	10	14.6	26.2
	S12363	20 °C	d_B	56.3	56.6	54.7
			d_W	12.9	15.6	19.3
		55 °C	d_B	48.1	49.5	48.9
			d_W	16.5	21.6	29.0

the drug, a slight increase was even seen as in DPPC/vinblastine mixtures hydrated with ammonium sulfate 150 mM at pH 5.3 [16,33]. It is likely that S12363, which was protonated in citrate buffer, was rather adsorbed at the lipid–water interface, interacting with the headgroups, than embedded in the bilayer.

X-ray patterns supported this hypothesis. At 20 °C, ESM bilayer exhibited a ripple lamellar gel phase, with a broad reflection at 4.17 Å, as previously observed in water. This Pβ′ long-range organization was not affected by the presence of the drug but the lamellar d-spacing was increased from 68 Å to 74.7 Å and the ripple length was decreased from 137 Å to113 Å (Fig. 10A). When temperature increased, the chain melting was evidenced by the 4.17 Å-WAXS line vanishing. At 55 °C, the lamellar d-spacing of the L_α phase was increased from 66.2 to 74.1 Å when the drug was added, due to an increase in d_W.

In the presence of 10 mol% of cholesterol, S12363 induced a decrease of T_{onset} but less than in water. The fusion enthalpy was slightly higher in the presence of S12363, whereas the peak was divided into two endotherms. The lamellar organization was not affected by the drug presence (Fig. 10B). Nevertheless, lamellar d-spacings were more influenced in citrate buffer than in water since a decrease of 4 Å was seen in the L_β phase at 20 °C and an increase of 5 Å was seen in the L_α phase at 55 °C. These variations were mainly due to variation of the water layer thickness (Table 1). The shapes of the electron density profiles seemed similar regardless the presence or the absence of the drug and whatever the temperature (Fig. 9C and D). However, the difference of the electron density between the center of

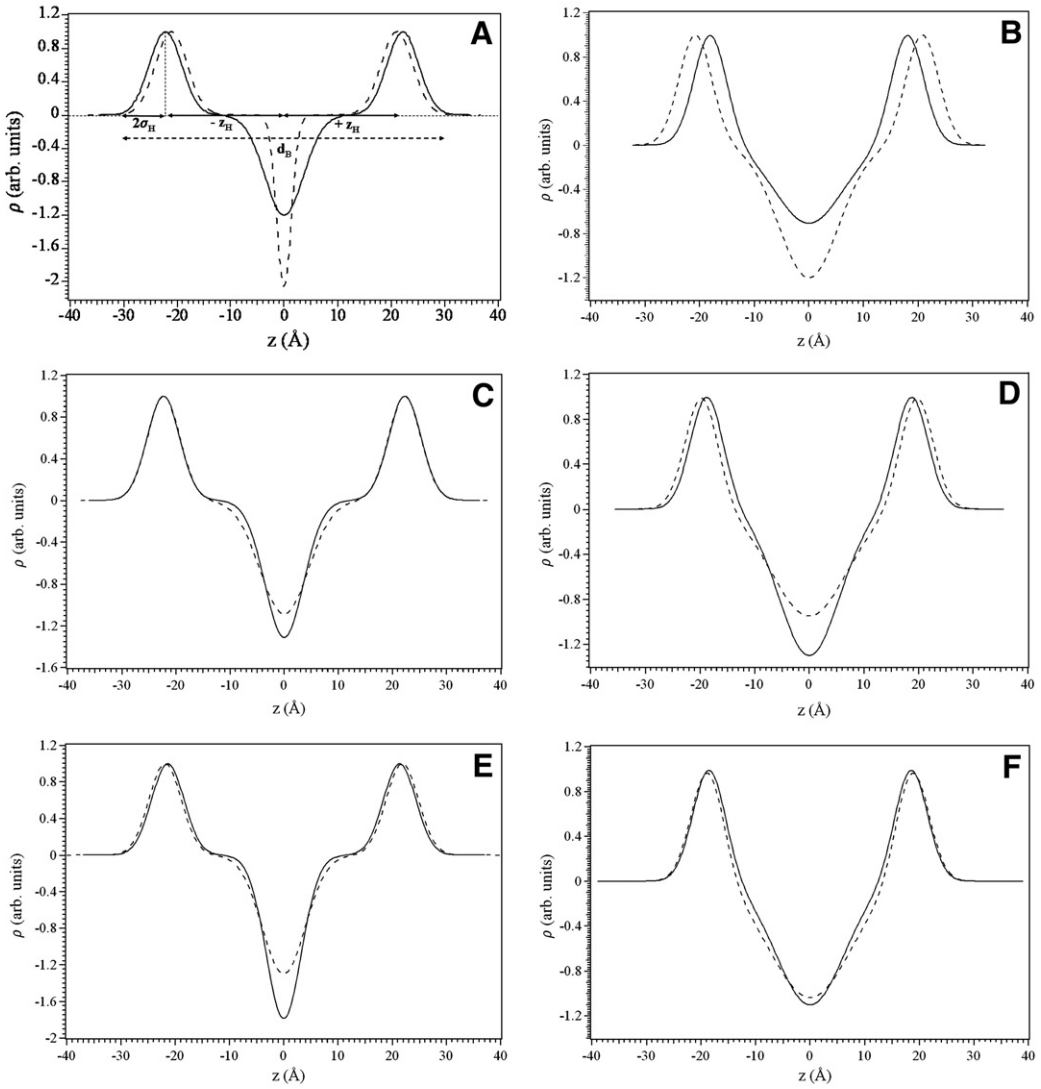

Fig. 9. One-dimensional electron density profile calculated from the small-angle scattering diffraction pattern exhibited by ESM/Chol (90:10) bilayers without S12363 (dash curves) or with S12363 (plain curves) fully hydrated with water (A, B), citrate buffer pH4 (C, D), and ammonium sulfate pH 4 (E, F) at 20 °C (A, C, E) and 55 °C (B, D, F). The Gaussians centered at $+/-z_H$ characterize the position of the headgroup and $2\sigma_H$ is its width. The bilayer thickness dB is defined by $dB = 2(z_H + 2\sigma_H)$, and the water layer dW is then given by $d_W = d - d_B$.

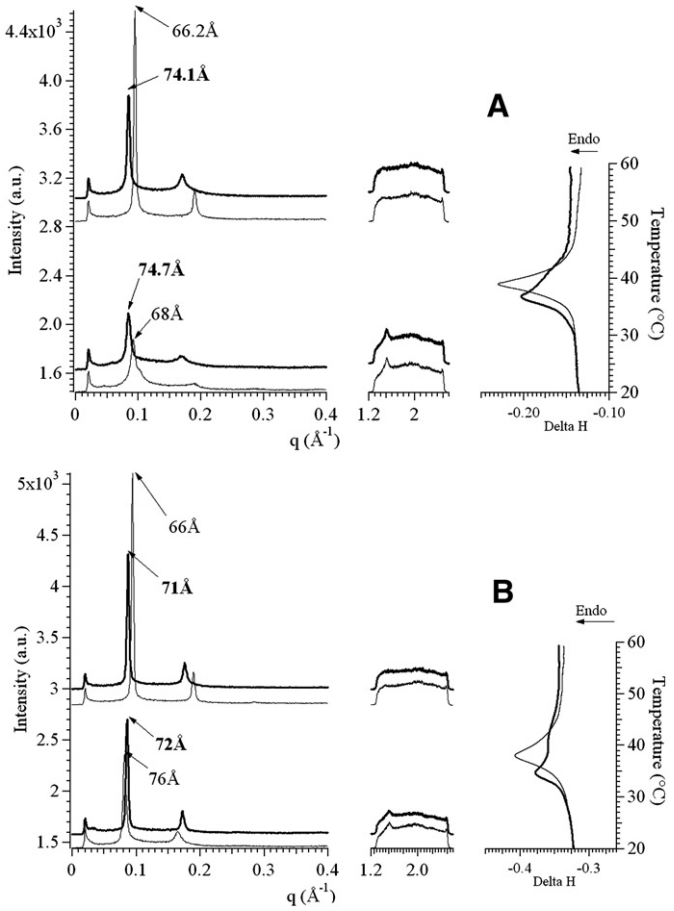

Fig. 10. SWAXS diffraction patterns (left) at 20 °C (bottom) and 55 °C (top) of bilayers hydrated with citrate buffer pH 4. (A) ESM bilayers (plain curves) or ESM/S12363 bilayers (bold curves) (B) ESM/Chol (90:10) bilayers (plain curves) or ESM/Chol/S12363 bilayers (bold curves). The right part shows corresponding DSC curves (scanning rate 2 °C/min).

the bilayer and the headgroup region at the water layer interface increased a little in the presence of the drug. As the center of the bilayer was supposed to have the same electron density in the conditions studied, variations observed between the center of the bilayer and the headgroup region should be due to modification of the headgroup electron density. This phenomenon confirms that the drug was mainly located at the interface and in the aqueous medium.

3.3.3. Drug/liposomes interactions in ammonium sulfate

The drug/bilayer interactions in ammonium sulfate appeared as intermediate between those observed in water and in citrate buffer. DSC measurements showed that T_{onset} was decreased and that the peak was broader, as in other cases; the fusion enthalpy was weakly decreased in the presence of the drug. As shown in a previous study, ESM bilayers in ammonium sulfate exhibited a disordered lamellar gel phase. The addition of S12363, like that of cholesterol, led to an organized lamellar gel phase with a 4.17 Å-WAXS line (Fig. 11A). In the liquid crystalline phase L_α, an increase of d-spacing (+3.8 Å) was seen in the presence of the drug. The decrease of T_m and ΔH and the effect on the lamellar gel phase organization showed that S12363 interacted with the lipid membrane and could be embedded. However, ΔH was not decreased as much as it was when the drug was inserted into the bilayer hydrated with water. In ammonium sulfate solution, as electrostatic interactions may exist between the amino group of S12363 and the negatively charged phosphate group, the drug inserted in the bilayer was, therefore, probably close to the interface.

In the presence of 10 mol% of cholesterol, the drug induced a decrease of T_{onset} and the very broad peak was divided into two endotherms whereas the fusion enthalpy was slightly decreased. The L_β organization was not affected by the drug but an important decrease of the lamellar d-spacing was observed (−9 Å) (Fig. 11B). Above the melting temperature, the lamellar d-spacing of the sample containing the drug was closer to that of ESM/Chol bilayers alone (+2 Å). Electron density profiles indicated that d-spacing changes arised mainly from water layer thickness (Table 1). Moreover, they also showed that at 20 °C, S12363 modified the difference of the electron density between the center of the bilayer and the headgroups

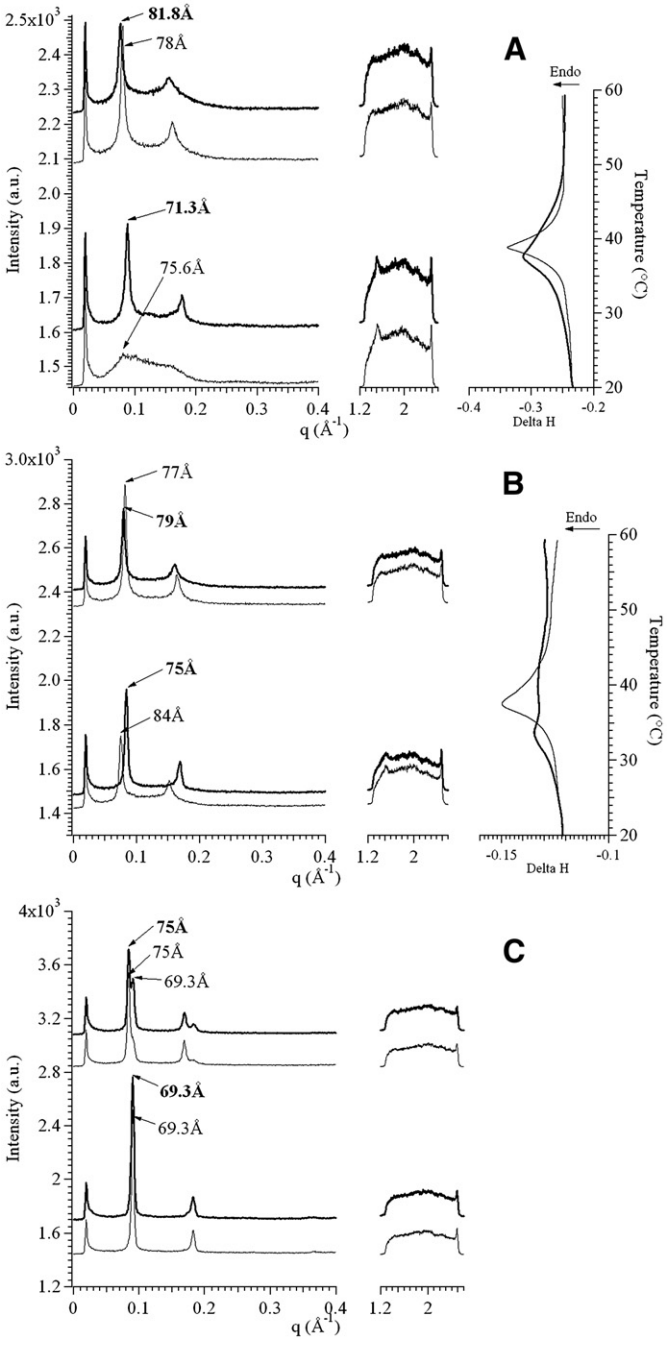

Fig. 11. SWAXS diffraction patterns (left) at 20 °C (bottom) and 55 °C (top) of bilayers hydrated with ammonium sulfate pH 4. (A) ESM bilayers (plain curves) or ESM/S12363 bilayers (bold curves) (B) ESM/Chol (90:10) bilayers (plain curves) or ESM/Chol/S12363 bilayers (bold curves). (C) ESM/Chol (60:40) bilayers (plain curves) or ESM/Chol/S12363 bilayers (bold curves). The right part shows corresponding DSC curves (scanning rate 2 °C/min).

Table 2
Encapsulation fraction of S12363 after 1 month at +4 °C and after S12363-liposomes dilution in PBS pH 7.4 at 37 °C during 30 min.

	Encapsulation fraction (%)	
	1 month 4 °C	Dilution 1:100
pH gradient	94 ± 6	67 ± 4
Ammonium gradient	94 ± 2	81 ± 3

Results are the average of 3 experimental data.

as already seen in citrate buffer. Surprisingly, this phenomenon was less marked at 55 °C.

In the presence of 40 mol% of cholesterol, the WAXS line as well as the calorimetric transition vanished. At 20 °C, the drug did not influence the membrane organization and the lamellar repeat period was unchanged (Fig. 11C). At 55 °C, the same behavior was seen but the drug presence favored the phase separation observed without the drug.

In all the conditions studied, the DSC curve shape suggested that the drug repartition into the membrane was not homogeneous. However, X-ray patterns showed only one well defined line corresponding to one lamellar phase. It is rather considered that inhomogeneities in the bilayer plan were formed, leading to S12363 rich domain specifically occurring in the presence of Chol (Chol-S12363 rich domains). The association between Chol and the drug could be steric (favored by complementary structures) and/or more specific depending on the charge. In any case, Chol is supposed to promote the drug insertion at least in the gel phase.

3.4. Liposome stability

Liposome stability was evaluated after 1 month at 4 °C. As shown in Table 2 both formulations were stable over this period.

The drug leakage was then determined (37 °C; PBS) after drug loading by either pH gradient or ammonium gradient. After 30 min, 67% (pH gradient) or 81% (ammonium gradient) of S12363 were still encapsulated (Table 2). Thus, the drug release was faster when the drug was encapsulated using a pH gradient rather than an ammonium gradient. The presence of the drug into the bilayer did not lead to a burst effect. On the contrary, drug–membrane interactions may favor the drug retention into the liposomes. Thus, when the drug was solubilized into the liposome core, it was released by a passive diffusion through the lipid bilayer after liposome dilution. This phenomenon was already observed in vinca-alcaloid loaded liposomes using a pH gradient [31]. Moreover, it was previously shown that the presence of sulfate into the liposome core could improve Topotecan encapsulation, due to drug precipitation [30]. In the case of S12363 encapsulated into liposomes by the ammonium gradient, a slight precipitation, not seen by cTEM, could explain the limited release observed. Furthermore, it has been previously shown that ammonium sulfate adsorbed at ESM/Chol membrane surface [32]. Thus, sulfate is likely enhancing interactions between S12363 and the bilayer, leading to a more stable formulation.

4. Conclusion

Interactions of the S12363 drug with ESM or ESM/Chol membranes have been investigated in water, ammonium sulfate solution and citrate buffer. It has been shown that, depending on the aqueous medium, S12363 may be deeply embedded within the bilayer, inserted in the vicinity of the polar headgroup or adsorbed at the water–lipid interface. When the bilayers were hydrated with water, insertion of the neutral S12363 was driven by hydrophobic interaction. In ammonium sulfate, positively charged amino groups of S12363 interacted with negatively charged phosphate groups, the lipophilic groups being oriented towards the hydrophobic part of the bilayer. When the membrane was melted, the lipid molecules became less ordered, leading to a better insertion of the drug into the bilayer. In citrate buffer, S12363 exhibited enhanced partitioning at the interface, probably because of a higher charge. Moreover, DSC studies have shown that the drug partitioning into the membrane was inhomogeneous and led to the formation of drug-rich and drug-poor domains. This effect was more marked when cholesterol was added, especially in ammonium sulfate.

Regarding interactions evidenced between the drug and the membrane bilayer, the supramolecular organization of the liposome membrane was supposed to be affected by the drug. The drug loading process and more specifically the formulation medium significantly influenced the drug/bilayer interactions. For both formulations, the encapsulated drug partitioned between the aqueous core and the bilayer. It was localized in the vicinity of the ESM polar head groups and partially embedded into the sphingomyelin tails. In the case of ammonium sulfate gradient, the drug was less soluble in the liposome core and drug/membrane interactions were favored, leading to more drug insertion into the bilayer and also to greatest stability of the liposome formulation. This study also showed that X-ray diffraction coupled to DSC is a useful tool for determining the localization of drugs into liposomes.

References

[1] G. Gregoriadis, E.J. Wills, C.P. Swain, A.S. Tavill, Drug-carrier potential of liposomes in cancer chemotherapy, Lancet 1 (1974) 1313–1316.
[2] G. Lavielle, P. Hautefaye, C. Schaeffer, J. Boutin, C. Cudennec, A. Pierre, New alpha-amino phosphonic acid derivatives of vinblastine: chemistry and antitumor activity, J. Med. Chem. 34 (1991) 1998–2003.
[3] A. Pierre, L. Kraus-Berthier, G. Atassi, S. Cros, M.F. Poupon, G. Lavielle, M. Berlion, J.P. Bizzari, Preclinical antitumor activity of a new Vinca alkaloid derivative, S 12363, Cancer Res. 51 (1991) 2312–2318.
[4] D.D. Lasic, Liposomes: From Physics to Applications, London, 1993.
[5] A. Chonn, P.R. Cullis, Recent advances in liposomal drug delivery systems, Curr. Opin. Biotechnol. 6 (1995) 698–708.
[6] L.D. Mayer, T.D. Madden, M.B. Bally, P.R. Cullis, pH Gradient-Mediated Drug Entrapment in Liposome, Vol. 2, CRC Press, Boca Raton, FL, 1993.
[7] E. Maurer-Spurej, K.F. Wong, N. Maurer, D.B. Fenske, P.R. Cullis, Factors influencing uptake and retention of amino-containing drugs in large unilamellar vesicles exhibiting transmembrane pH gradients, Biochim. Biophys. Acta 1416 (1999) 1–10.
[8] D. Needham, R.S. Nunn, Elastic deformation and failure of lipid bilayer membranes containing cholesterol, Biophys. J. 58 (1990) 997–1009.
[9] O.G. Mouritsen, K. Jorgensen, Dynamical order and disorder in lipid bilayers, Chem. Phys. Lipids 73 (1994) 3–25.
[10] O.G. Mouritsen, K. Jorgensen, A new look at lipid–membrane structure in relation to drug research, Pharm. Res. 15 (1998) 1507–1519.
[11] M.S. Webb, M.B. Bally, L.D. Mayer, J.J. Miller, P.G. Gardi. Vol. 05, pp. 335, Inex Pharmaceuticals Corporation, U.S. 1998.
[12] S.C. Semple, R. Leone, J. Wang, E.C. Leng, S.K. Klimuk, M.L. Eisenhardt, Z.-N. Yuang, K. Edwards, N. Maurer, M.J. Hope, P.R. Cullis, Q.F. Ahkong, Optimization and characterization of sphingomyelin/cholesterol liposome formulation of vinorelbine with promising antitumor activity, J. Pharm. Sci. 94 (2005) 1024–1038.
[13] S. Amselem, R. Cohen, Y. Barenholz, In vitro tests to predict in vivo performance of liposomal dosage forms, Chem. Phys. Lipids 64 (1993) 219–237.
[14] G.J.R. Charrois, T.M. Allen, Drug release rate influences the pharmacokinetics, biodistribution, therapeutic activity, and toxicity of pegylated liposomal doxorubicin formulations in murine breast cancer, Biochim. Biophys. Acta (BBA) – Biomembranes 1663 (2004) 167–177.
[15] G.E. Flaten, M. Skar, K. Luthman, M. Brandl, Drug permeability across a phospholipid vesicle based barrier: 3. Characterization of drug–membrane interactions and the effect of agitation on the barrier integrity and on the permeability, Eur. J. Pharm Sci. 30 (2007) 324–332.
[16] I. Kyrikou, I. Daliani, T. Mavromoustakos, H. Maswadeh, C. Demetzos, S. Hatziantoniou, S. Giatrellis, G. Nounesis, The modulation of thermal properties of vinblastine by cholesterol in membrane bilayers, Biochim. Biophys. Acta 1661 (2004) 1–8.
[17] R. Nicholov, V. DiTizio, F. DiCosmo, Interaction of paclitaxel with phospholipid bilayers, J. Liposome Res. 5 (1995) 503–522.
[18] D.J. Siminovitch, M.J. Ruocco, A. Makriyannis, R.G. Griffin, The effect of cholesterol on lipid dynamics and packing in diether phosphatidylcholine bilayers. X-ray diffraction and ^{2}H-NMR study, Biochim. Biophys. Acta 901 (1987) 191–200.
[19] C. Grabielle-Madelmont, A. Hochapfel, M. Ollivon, Antibiotic–phospholipid interactions as studied by DSC and X-ray diffraction, J. Phys. Chem 103 (1999) 4534–4548.
[20] H.-J. Lin, H. Szmacinski, J.R. Lakowicz, Lifetime-based pH sensors: indicators for acidic environments, Anal. Biochem. 269 (1999) 162–167.
[21] C. Grabielle-Madelmont, R. Perron, Calorimetric studies on phospholipids-water systems. I. DL-dipalmitoylphosphatidylcholine (DPPC)–water system, J. Colloid Interface Sci. 95 (1983) 471–482.

[22] G. Keller, F. Lavigne, L. Forte, K. Andrieux, M. Dahim, C. Loisel, M. Ollivon, C. Bourgaux, P. Lesieur, DSC and X-ray diffraction coupling specifications and applications, J. Therm. Anal. Calorim. 51 (1998) 783–791.
[23] F. Lavigne, C. Bourgaux, M. Ollivon, Phase transitions of saturated triglycerides, J. Phys. IV 3 (1993) 137–140.
[24] G. Pabst, M. Rappolt, H. Amenitsch, P. Laggner, Structural information from multilamellar liposomes at full hydration: full *q*-range fitting with high quality X-ray data, Phys. Rev. E 62 (2000) 4000–4009.
[25] G. Pabst, R. Koschuch, B. Pozo-Navas, M. Rappolt, K. Lohner, P. Laggner, Structural analysis of weakly ordered membrane stacks, J. Appl. Cryst. 36 (2003) 1378–1388.
[26] G. Pabst, Global properties of biomimetic membranes: perspectives on molecular features, Biophys. Rev. Lett. 1 (2006) 57–84.
[27] M.J. Hope, M.B. Bally, G. Webb, P.R. Cullis, Production of large unilamellar vesicule by a rapid extrusion procedure. Characterisation of size distribution, trapped volume and ability to maintain a membrane potential, Biochim. Biophys. Acta 812 (1985) 55–65.
[28] P.R. Cullis, M.J. Hope, M.B. Bally, T.D. Madden, L.D. Mayer, A.S. Janoff, Liposomes as pharmaceuticals, in: M.J. Ostro (Ed.), Liposomes From Biophysics to Therapeutics, Marcel Dekker, New York, 1987, pp. 39–72.
[29] D.D. Lasic, B. Ceh, M.C.A. Stuart, L. Guo, P.M. Frederik, Y. Barenholz, Transmembrane gradient driven phase transitions within vesicles: lessons for drug delivery, Biochim. Biophys. Acta (BBA) – Biomembranes 1239 (1995) 145–156.
[30] S.A. Abraham, K. Edwards, G. Karlsson, N. Hudon, L.D. Mayer, M.B. Bally, An evaluation of transmembrane ion gradient-mediated encapsulation of topotecan within liposomes, J. Control. Release 96 (2004) 449–461.
[31] I.V. Zhigaltsev, N. Maurer, Q.-F. Akhong, R. Leone, E. Leng, J. Wang, S.C. Semple, P.R. Cullis, Liposome-encapsulated vincristine, vinblastine and vinorelbine: a comparative study of drug loading and retention, J. Control. Release 104 (2005) 103–111.
[32] C. Chemin, C. Bourgaux, J.-M. Péan, G. Pabst, P. Wüthrich, P. Couvreur, M. Ollivon, Consequences of ions and pH on the supramolecular organization of sphingomyelin and sphingomyelin/cholesterol bilayers, Chem. Phys. Lipids 153 (2008) 119–129.
[33] H. Maswadeh, C. Demetzos, I. Daliani, I. Kyrikou, T. Mavromoustakos, A. Tsortos, G. Nounesis, A molecular basis explanation of the dynamic and thermal effects of vinblastine sulfate upon dipalmitoylphosphatidylcholine bilayer membranes, Biochim.Biophys. Acta (BBA) – Biomembranes 1567 (2002) 49–55.